
Electronic supplementary information (ESI)

Guest-induced Reversible Crystal-to-Amorphous-to-Crystal Transformation in a Co(II) Based Metal Organic Framework

Huiling Tan, Qibin Chen*, Yujie Sheng, Xiaoxiao Li, Honglai Liu*

State Key Laboratory of Chemical Engineering and School of Chemistry & Molecular Engineering, East China University of Science and Technology, Shanghai, 200237, P.R. China

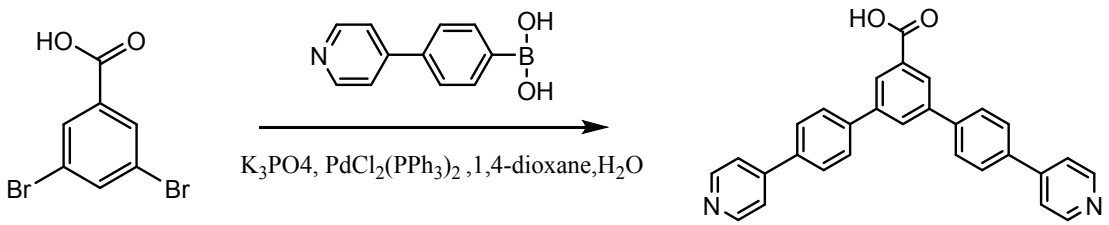

Scheme S1. Synthetic scheme for DPPB

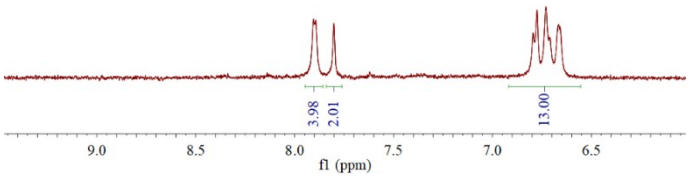

Fig S1. ^{1}H NMR spectrum of DPPB

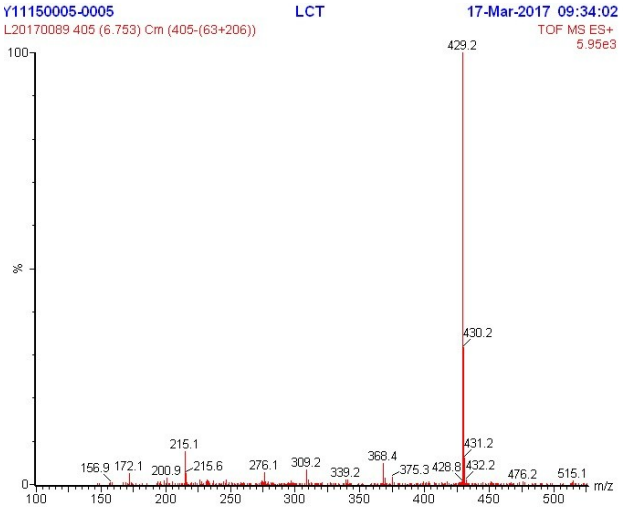

Fig S2. Mass spectrum of DPPB

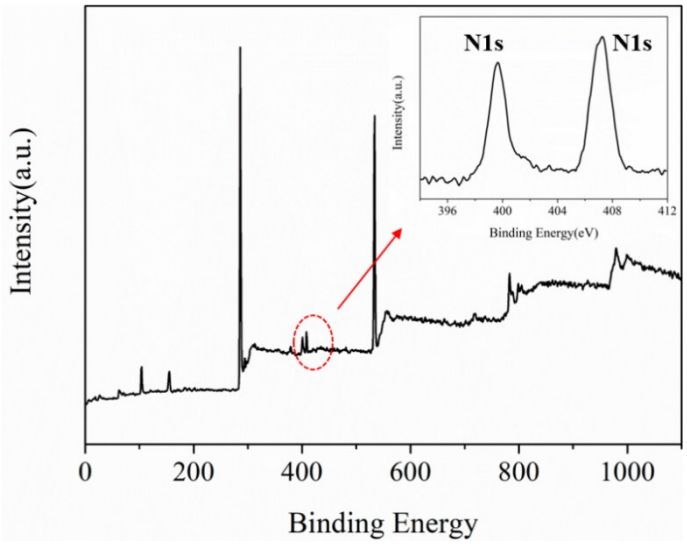

Fig S3. XPS spectra of DPPB-1

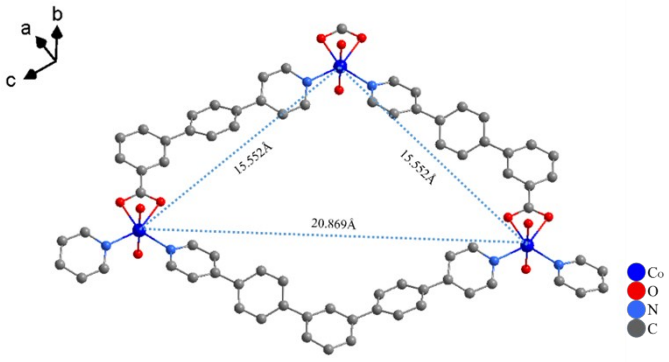

Fig S4. Honeycomb-like cavity showing the isosceles triangle formed by the three metal centers with the edge lengths (Co···Co separation) of 15.552 and 20.869Å.

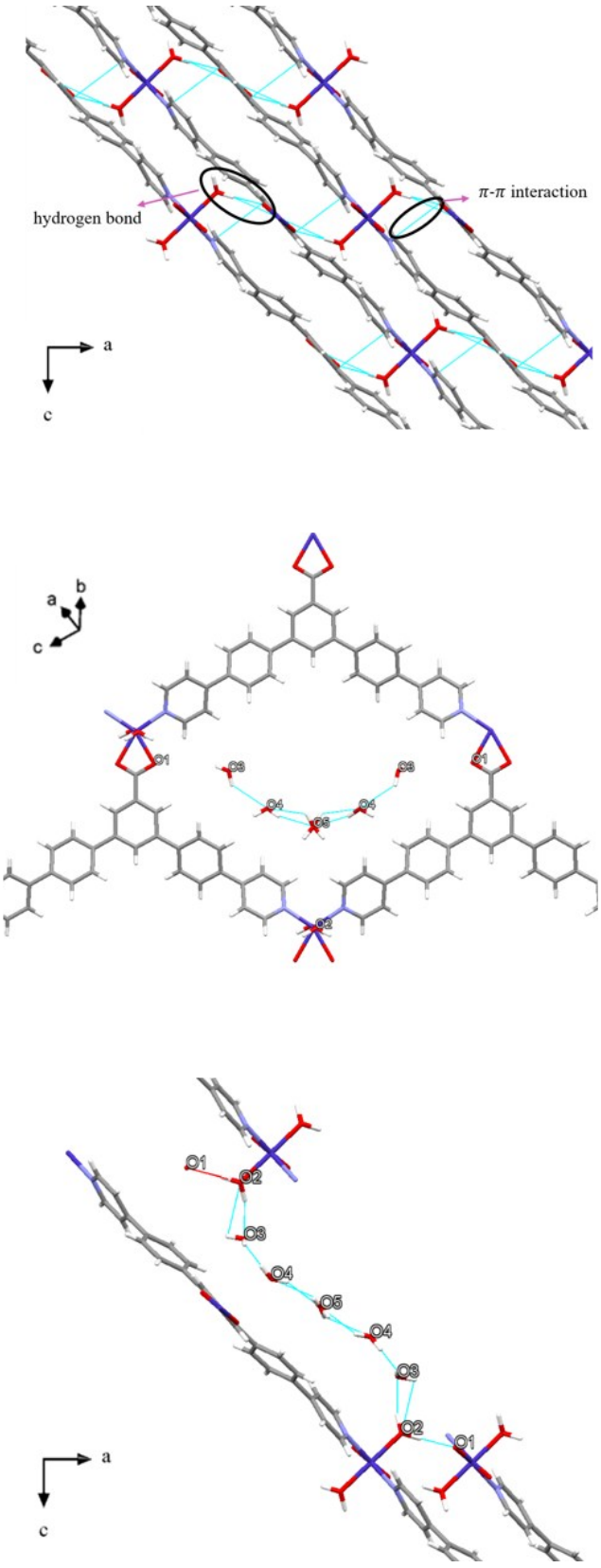

Fig S5. Structure view for DPPB-1 along the b axis (a) and c axis (b). Guests are omitted for clarity in a.

Color codes: Co, dark blue; N, light blue; C, grey; O, red.

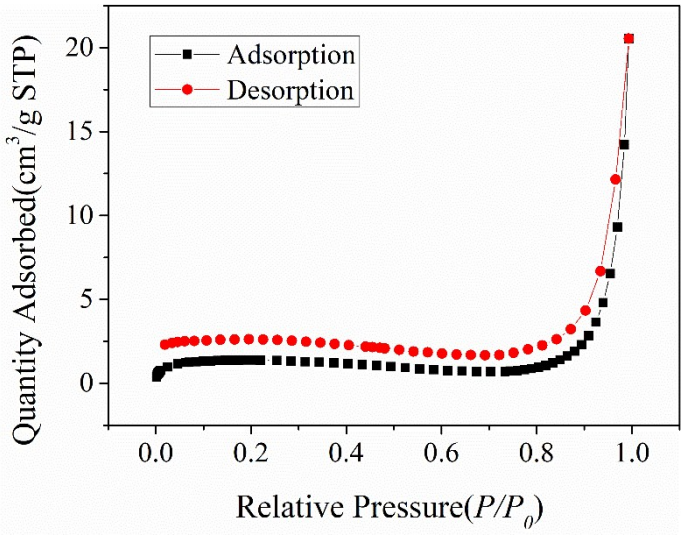

Fig S6. The N_2 adsorption-desorption isotherm of DPPB-2 at 77K

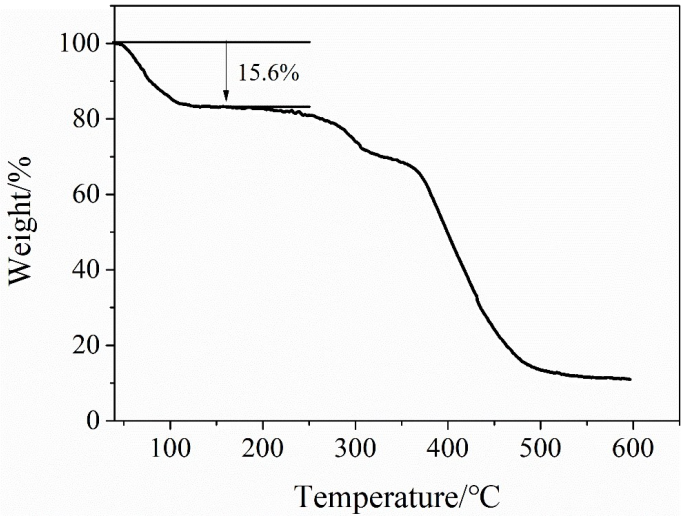

Fig S7. TGA curves of DPPB-1

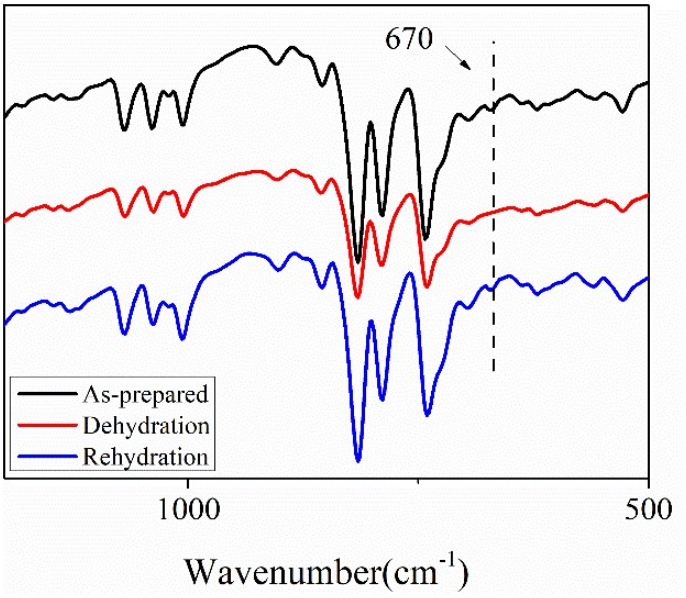

Fig S8. IR spectra of DPPB-1 during dehydration and rehydration

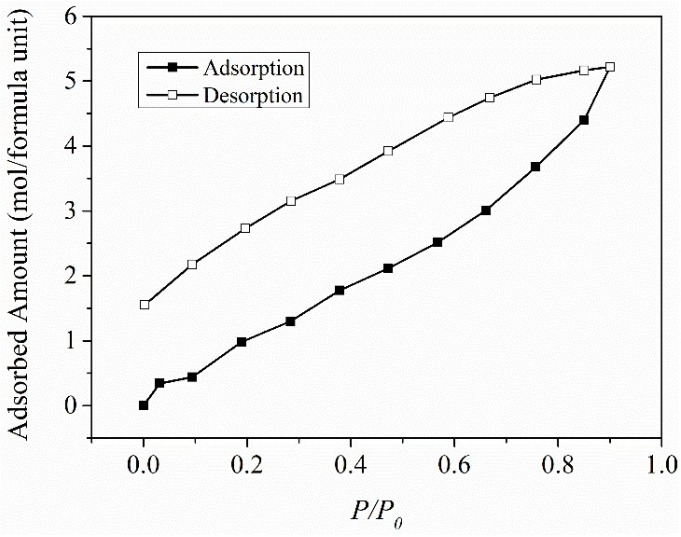

Fig S9. The ad/desorption isotherms of DPPB-2 for water at 298 K

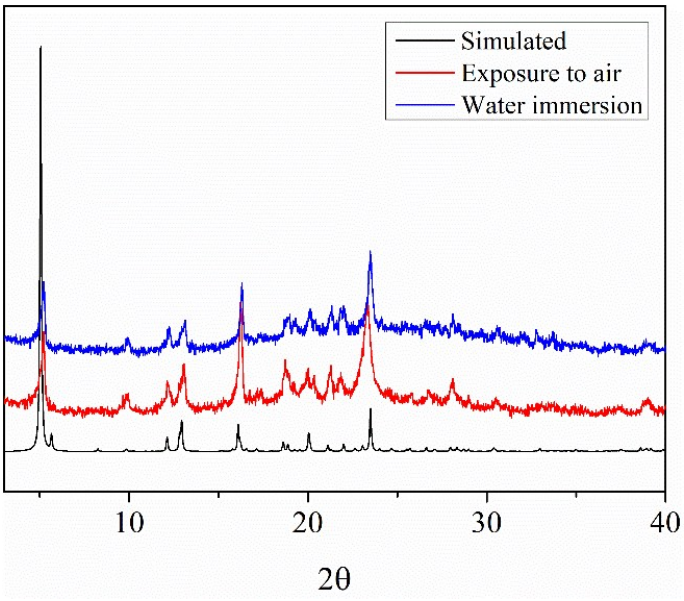

Fig S10. The PXRD pattern of DPPB-2 treated by water immersion and exposure to the air

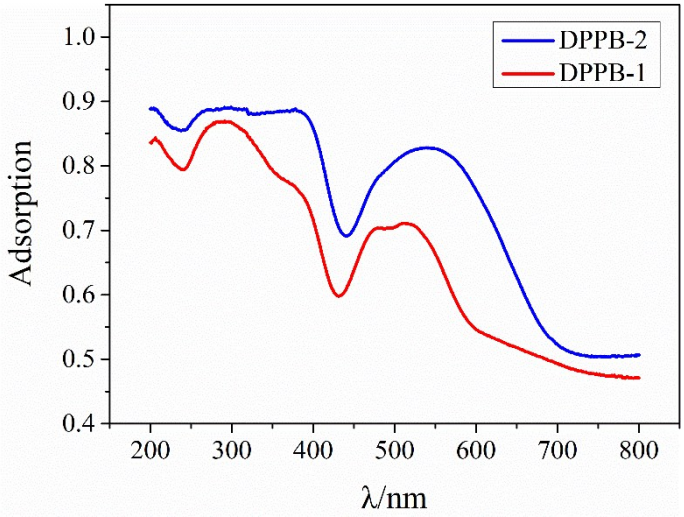

Fig S11. Solid UV-visible spectra of DPPB-1 and DPPB-2

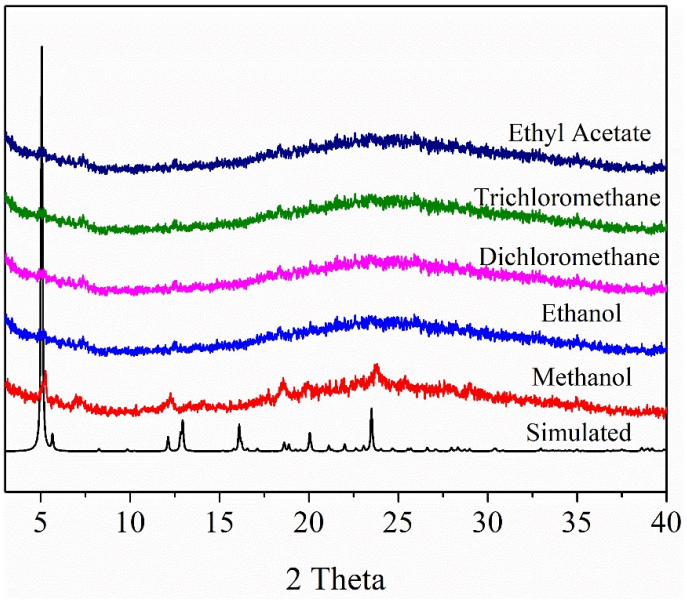

Fig S12. The PXRD patterns of DPPB-2 immersed in different solvent

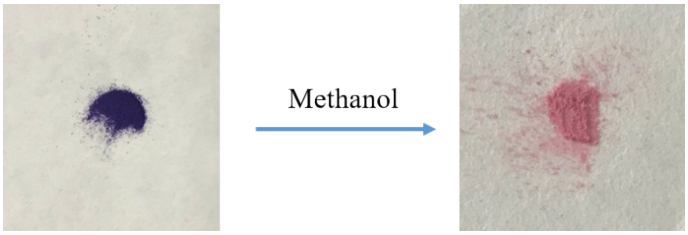

Fig S13. Color change of DPPB-2 in methanol

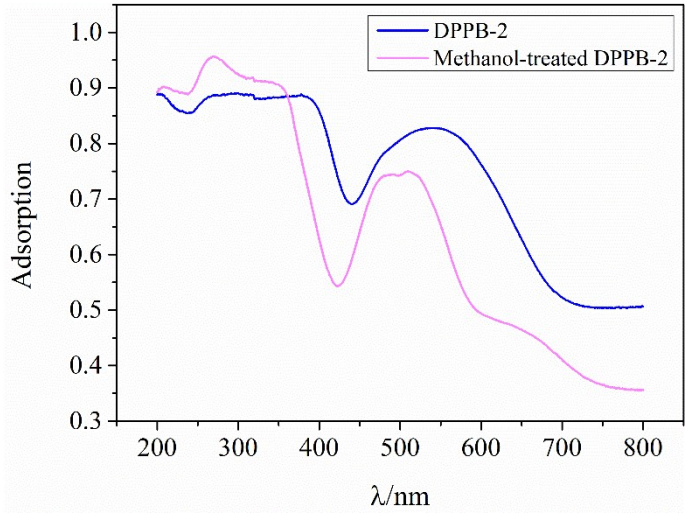

Fig S14. Solid UV-visible spectra of DPPB-2 and Methanol-treated DPPB-2

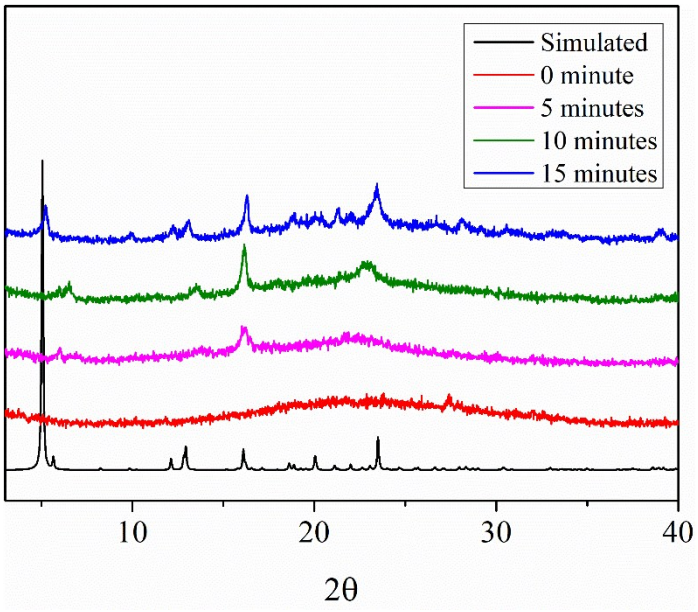

Fig S15. The PXRD patterns of DPPB-2 samples immersed in methanol.

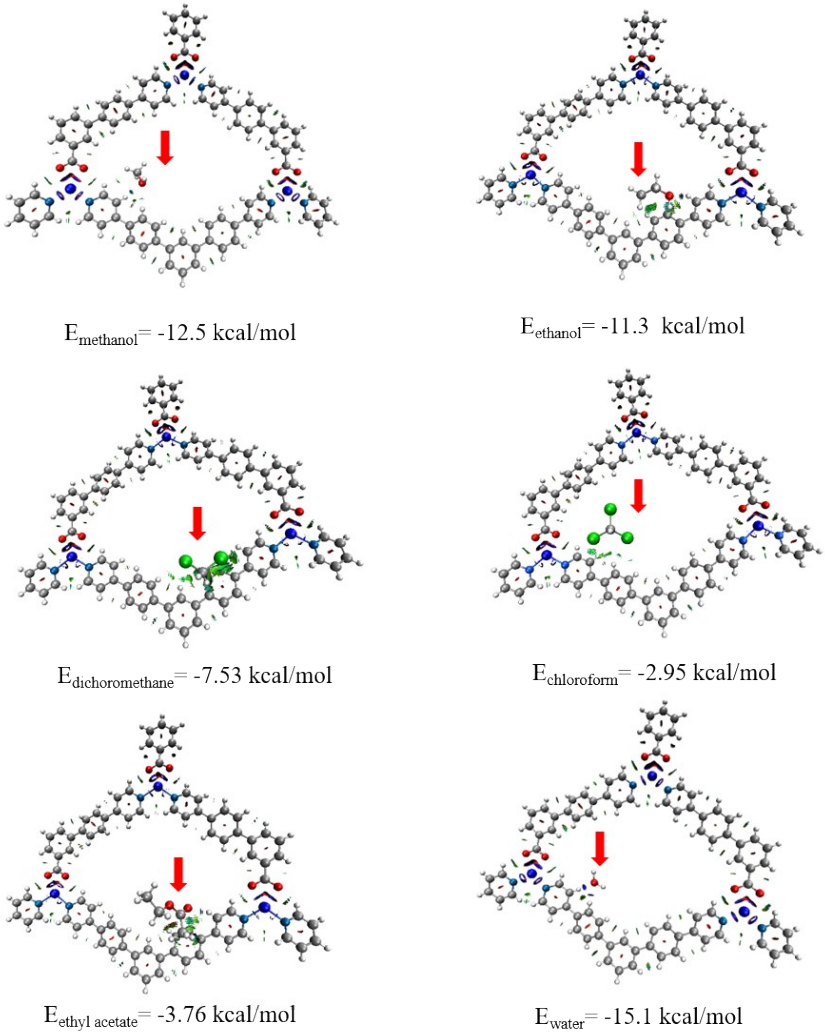

Fig *S16*. Energies and NCI analyses for host-guest interactions between guest molecules and cavity. VOC molecules are mark as red arrows.

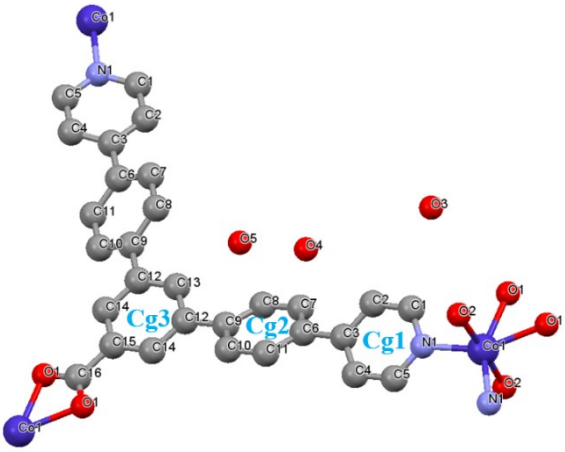

Fig S17. The asymmetric unit and atom labeling of scheme of DPPB-1. Guests and hydrogen atoms are omitted for clarity.

Table S1. Hydrogen bonds (Å, Deg.) calculated by PLATON software for DPPB-1.

Donor ---H....Acceptor	D - H	H...A	D...A	D - H...A
O(2)---H(1A)….O(3)	0.96	1.90	2.740	144
O(2)---H(2B)….O(1)	0.96	1.82	2.757	163
O(3)---H(3A)….O(4)	0.85	2.54	3.210	136
O(4)---H(4A)….O(5)	0.85	2.19	3.09	151

Table S2. Analysis of short ring-interactions with Cg-Cg Distances < 6.0 Å and Beta < 60.0 Deg. calculated by PLATON software for DPPB-1. Alpha: Dihedral Angle between Planes I and J (Deg); Beta: Angle Cg(I)--Cg(J) or Cg(I)--Me vector and normal to plane I (Deg); Gamma: Angle Cg(I)--Cg(J) vector and normal to plane J (Deg).

Cg(I)·····Cg(J)	D(Cg-Cg)	Alpha	Beta	Gamma
Cg(1)·····Cg(2)	5.330(2)	36	35.1	70.5
Cg(1)·····Cg(3)	3.7512(17)	14	29.2	16.7
Cg(1)·····Cg(3)	3.7512(17)	14	29.2	16.7
Cg(2)·····Cg(1)	5.778(3)	20	57.6	67.4
Cg(2)·····Cg(2)	3.7105(17)	0	18.3	18.3
Cg(2)·····Cg(3)	4.927(2)	22	2.3	47.5
Cg(2)·····Cg(3)	4.927(2)	22	42.3	47.5
Cg(3)·····Cg(1)	3.7512(17)	14	16.7	29.2
Cg(3)·····Cg(1)	3.7512(17)	14	16.7	29.2
Cg(3)·····Cg(2)	4.927(2)	22	47.5	42.3
Cg(3)·····Cg(2)	4.927(2)	22	47.5	42.3

Table S3. Methanol adsorption capacity of different materials

Material	Ligand	q_{max}(g/g)	ref
$Co(pybz)_2$	pybz	0.23	[1]
$Zn_2(BDC)_2(dabco)$	BDC/dabco	0.21	[2]
MAF-5(Zn)	eim	0.20	[3]
Cu2(dmcapz)2	dmcapz	0.19	[4]
$[Cd_2(pbpy)(bdc)_2Cl_2] \cdot 5H_2O$	pbpy/bdc	0.18	[5]
Al(OH)-(1,4-NDC)	1,4-NDC	0.16	[6]
$[Cd_2(pbpy)(bdc)_2ClBr] \cdot 9H_2O$	pbpy/bdc	0.16	[5]
$Zn_5O_2(bpdc)_4$	bpdc	0.15	[7]
ThrZnOAc	Thr	0.15	[8]
Zn(tbip)	Tbip	0.11	[9]
$Cu_2(pzdc)_2(dpyg)$	Pzdc/dpyg	0.11	[10]
CoDPE	DPE	0.11	[11]
$Co_3(fa)_6$	FA	0.10	[12]
$Zn_2(bptc)$	Bptc	0.10	[13]
$[Cd_2(pbpy)(bdc)_2Br_2] \cdot 8H_2O$	pbpy/bdc	0.10	[5]
DPPB-2	dppb	0.26	This work

Table S4. Ethanol adsorption capacity of different materials

Material	Ligand	q_{max}(g/g)	ref
MIL-100(Fe)	TPA	0.34	[14]
$Zn_2(BDC)_2(dabco)$	BDC/dabco	0.33	[2]
ZIF-8(Zn)	mIm	0.28	[15]
ZIF-71(Zn)	dcIm	0.28	[15]
ZIF-90(Zn)	Ica	0.28	[15]
ZIF-68(Zn)	nIm/bIm	0.26	[16]
([Eu(CAM) (HCAM)2Mn2(H2O)4])n	(H)CAM	0.26	[17]
$(H_2dab)[Zn_2(ox)_3]$	ox/dab	0.26	[18]
MAF-2(Cu)	etz	0.25	[19]
$Zn_2(NDC)_2(dabco)$	1,4-NDC/dabco	0.20	[2]
$[Cd_2(pbpy)(bdc)_2Cl_2] \cdot 5H_2O$	pbpy/bdc	0.19	[5]
$[Cd_2(pbpy)(bdc)_2ClBr] \cdot 9H_2O$	pbpy/bdc	0.16	[5]
Co3(fa)6	FA	0.14	[1]
$[Cd_2(pbpy)(bdc)_2Br_2] \cdot 8H_2O$	pbpy/bdc	0.088	[5]
$([Ni(L6)_2] \cdot 4H_2O)n$	L6	0.070	[20]
[Cd(L7) (DMF)]	L7	0.060	[21]
DPPB-2	dppb	0.37	This work

Table S5. The selectivity of DPPB-2 for VOCs at 298K

Type	Selectivity
$C_2H_5OH/CHCl_3$	21.5
C_2H_5OH/CH_2Cl_2	19.4
C_2H_5OH/EA	25.1
$CH_3OH/CHCl_3$	15.6
CH_3OH/CH_2Cl_2	14.7
CH_3OH/EA	16.2

Table S6. Crystal data and structure refinement parameters for DPPB-1 or [Co $(H_2O)_2$ (DPPB)] ·(NO_3) ·3.5H_2O

Formula	DPPB-1	□
Empirical formula	C29 H30 Co N2 O7.50	
Formula weight	585.48	
Temperature	296 K	
Wavelength	0.71073 Å	
Crystal system	Monoclinic	
Space group	C 1 2/c 1	
Unit cell dimensions	a = 15.715(7) Å	a= 90°.
	b = 23.065(9) Å	b= 108.308(7)°.
	c = 9.764(4) Å	g = 90°.
Volume	3360(2) Å3	
Z	4	
Density (calculated)	1.157 Mg/m3	
Absorption coefficient	0.553 mm-1	
F(000)	1220	
Crystal size	0.12 x 0.1 x 0.08 mm3	
Theta range for data collection	2.819 to 27.814°.	
Index ranges	-20<=h<=20, -30<=k<=27, -12<=l<=9	
Reflections collected	13526	
Independent reflections	3892 [R(int) = 0.0970]	
Completeness to theta = 25.242°	98.90%	
Absorption correction	Semi-empirical from equivalents	
Max. and min. transmission	0.7456 and 0.6495	
Refinement method	Full-matrix-block least-squares on F2	
Data / restraints / parameters	3892 / 18 / 198	
Goodness-of-fit on F2	0.884	
Final R indices [I>2sigma(I)]	R1 = 0.0606, wR2 = 0.1532	
R indices (all data)	R1 = 0.1297, wR2 = 0.1914	
Extinction coefficient	n/a	

Largest diff. peak and hole	0.550 and -0.464 e.Å-3

Table S7. Atomic coordinates (x 104) and equivalent isotropic displacement parameters (Å2x 103) for DPPB-1. U(eq) is defined as one third of the trace of the orthogonalized Uij tensor.

	x	y	z	U(eq)
Co(1)	10000	9458	12500	41(1)
O(1)	4522	5281	1415	44(1)
O(2)	9051	9430	13533	53(1)
N(1)	9137	8950	10860	44(1)
C(1)	8429	9215	9913	62(1)
C(2)	7840	8925	8766	60(1)
C(3)	7954	8339	8548	44(1)
C(4)	8670	8073	9534	46(1)
C(5)	9249	8381	10651	47(1)
C(6)	7345	8027	7294	43(1)
C(7)	6982	8303	5959	55(1)
C(8)	6442	8004	4778	51(1)
C(9)	6215	7426	4900	38(1)
C(10)	6571	7152	6224	46(1)
C(11)	7131	7446	7395	48(1)
C(12)	5608	7111	3645	36(1)
C(13)	5000	7396	2500	38(1)
C(14)	5609	6506	3600	37(1)
C(15)	5000	6202	2500	32(1)
C(16)	5000	5557	2500	35(1)
O(3)	7226	10470	7413	231(4)
O(4)	5934	8572	10422	202(6)
O(5)	5000	8118	7500	141(5)

Table S8. Selected bonds lengths (Å) for DPPB-1

Bond lengths	Å	Bond lengths	Å
Co(1)-O(1)	2.19	O(1)-C(16)	1.26
Co(1)-O(2)	2.05	O(2)-H(2A)	0.96
Co(1)-N(1)	2.1	O(2)-H(2B)	0.96
		N(1)-C(1)	1.35
		N(1)-C(5)	1.35
		C(1)-H(1)	0.93
□	□	C(1)-C(2)	1.38

Reference

(1) Zeng, M. H.; Tan, Y. X.; He, Y. P.; Yin, Z.; Chen, Q.; Kurmoo, M., A porous 4-fold-interpenetrated chiral framework exhibiting vapochromism, single-crystal-to-single-crystal solvent exchange, gas sorption, and a poisoning effect. *Inorg. Chem* **2013,** 52, (5), 2353-2360.

(2) Uemura, K.; Komagawa, Y.; Yamasaki, Y.; Kita, H., Characterization of organic solvents adsorption/desorption on hydrophobic porous coordination polymers and their micro-crystals aggregation on mullite support. *Desalination* **2008,** 234, (1–3), 1-8.

(3) Zhu, A. X.; Lin, R. B.; Qi, X. L.; Liu, Y.; Lin, Y. Y.; Zhang, J. P.; Chen, X. M., Zeolitic metal azolate frameworks (MAFs) from ZnO/Zn(OH) 2 and monoalkyl-substituted imidazoles and 1,2,4-triazoles: Efficient syntheses and properties. *Microporous Mesoporous Mater* **2012,** 157, (27), 42-49.

(4) Quartapelle Procopio, E.; Fukushima, T.; Barea, P. E.; Navarro, P. J. A. R.; Horike, P. S.; Kitagawa, P. S., A Soft Copper(II) Porous Coordination Polymer with Unprecedented Aqua Bridge and Selective Adsorption Properties. *Chem. - Eur. J* **2012,** 18, (41), 13117-13125.

(5) Chen, C.; Cai, L. X.; Tan, B.; Zhang, Y. J.; Yang, X. D.; Lin, S.; Zhang, J., Flexible Bipyridinium Constructed Porous Frameworks with Superior Broad-Spectrum Adsorption toward Organic Pollutants. *Cryst. Growth Des* **2017,** 17, (4), 1843-1848.

(6) Comotti, A.; Bracco, S.; Sozzani, P.; Horike, S.; Matsuda, R.; Chen, J.; Takata, M.; Kubota, Y.; Kitagawa, S., Nanochannels of two distinct cross-sections in a porous Al-based coordination polymer. *J. Am. Chem. Soc* **2008,** 130, (41), 13664-13672.

(7) Fang, Q. R.; Zhu, G. S.; Jin, Z.; Xue, M.; Wei, X.; Wang, D. J.; Qiu, S. L., A Novel Metal−Organic Framework with the Diamondoid Topology Constructed from Pentanuclear Zinc-Carboxylate Clusters. *Cryst. Growth Des* **2007,** 7, (6), 1035-1037.

(8) Kundu, T.; Sahoo, S. C.; Banerjee, R., Relating pore hydrophilicity with vapour adsorption capacity in a series of amino acid based metal organic frameworks. *CrystEngComm* **2013,** 15, (45), 9634-9640.

(9) Olson, D. H.; Parker, B., Zn(tbip) (H2tbip = 5-tert-Butyl lsophthalic Acid): A Highly Stable Guest-Free Microporous Metal Organic Framework with Unique Gas Separation Capability. *J. Am. Chem. Soc* **2006,** 128, (13), 4180-4181.

(10) Kitaura, R.; Fujimoto, K.; Noro, S.; Kondo, M.; Kitagawa, S., A pillared-layer coordination polymer network displaying hysteretic sorption: [Cu(2)(pzdc)(2)(dpyg)](n) (pzdc= pyrazine-2,3-dicarboxylate; dpyg=1,2-Di(4-pyridyl)glycol). *Angew. Chem., Int. Ed* **2002,** 41, (1), 133-135.

(11) Hou, C.; Liu, Q.; Okamura, T.; Wang, P.; Sun, W. Y., Dynamic porous metal-organic frameworks: synthesis, structure and sorption property. *CrystEngComm* **2012,** 14, (24), 8569-8576.

(12) Li, K.; Olson, D. H.; Lee, J. Y.; Bi, W.; Wu, K.; Yuen, T.; Xu, Q.; Li, J., Multifunctional Microporous MOFs Exhibiting Gas/Hydrocarbon Adsorption Selectivity, Separation Capability and Three-Dimensional Magnetic Ordering. *Adv. Funct. Mater* **2010,** 18, (15), 2205-2214.

(13) Lin, X.; Blake, A. J.; Wilson, C.; Sun, X. Z.; Champness, N. R.; George, M. W.; Hubberstey, P.; Mokaya, R.; Schröder, M., A porous framework polymer based on a zinc(II) 4,4'-bipyridine-2,6,2',6'-tetracarboxylate: synthesis, structure, and "zeolite-like" behaviors. *J. Am. Chem. Soc* **2006,** 128, (33), 10745-10753.

(14) Seo, Y. K.; Ji, W. Y.; Ji, S. L.; Lee, U. H.; Hwang, Y. K.; Jun, C. H.; Horcajada, P.; Serre, C.; Chang, J. S., Large scale fluorine-free synthesis of hierarchically porous iron(III) trimesate MIL-100(Fe) with a zeolite MTN topology. *Microporous Mesoporous Mater* **2012,** 157, (27), 137-145.

(15) Zhang, K.; Lively, R. P.; Dose, M. E.; Brown, A. J.; Zhang, C.; Chung, J.; Nair, S.; Koros, W. J.; Chance, R. R., Alcohol and water adsorption in zeolitic imidazolate frameworks. *Chem. Commun* **2013,**

49, (31), 3245-3257.

(16) Van, d. P. S.; Van, A. T.; Bozbiyik, B.; Lannoeye, J.; De Vos, D. E.; Baron, G. V.; Denayer, J. F., Adsorptive characterization of the ZIF-68 metal-organic framework: a complex structure with amphiphilic properties. *Langmuir* **2014,** 30, (28), 8416-8424.

(17) Z, N.; S, F.; JG, M.; XP, Z.; P, C., Enhancement of adsorption selectivity for MOFs under mild activation and regeneration conditions. *Chem. Commun* **2014,** 50, (58), 7797-7799.

(18) Sadakiyo, M.; Yamada, T.; Kitagawa, H., Hydroxyl group recognition by hydrogen-bonding donor and acceptor sites embedded in a layered metal-organic framework. *J. Am. Chem. Soc* **2011,** 133, (29), 11050-11053.

(19) Zhang, J. P.; Chen, X. M., Exceptional framework flexibility and sorption behavior of a multifunctional porous cuprous triazolate framework. *J. Am. Chem. Soc* **2008,** 130, (18), 6010-6017.

(20) Hou, C.; Liu, Q.; Wang, P.; Sun, W. Y., Porous metal-organic frameworks with high stability and selective sorption for CO 2 over N2 . *Microporous Mesoporous Mater* **2013,** 172, (172), 61-66.

(21) Huang, Y.; Zheng, X.; Duan, J.; Liu, W.; Zhou, L.; Wang, C.; Wen, L.; Zhao, J.; Li, D., A highly stable multifunctional three-dimensional microporous framework: excellent selective sorption and visible photoluminescence. *Dalton Trans* **2014,** 43, (18), 6811-6818.